Geophysical Research Letters

RESEARCH LETTER
10.1029/2019GL084015

A New Perspective on Terrestrial Hydrologic Intensity That Incorporates Atmospheric Water Demand

Darren L. Ficklin[1], John T. Abatzoglou[2], and Kimberly A. Novick[3]

[1]Department of Geography, Indiana University, Bloomington, IN, USA, [2]Department of Geography, University of Idaho, Moscow, ID, USA, [3]O'Neill School of Public and Environmental Affairs, Indiana University, Bloomington, IN, USA

Key Points:
- We develop a hydrologic intensity metric that incorporates daily supply and demand using precipitation and reference evapotranspiration
- Widespread hydrologic intensification occurred over the past four decades and will continue into the future
- Adding demand couples intensity metrics to ecohydrologic conditions and produces greater increases than metrics with static demand

Supporting Information:
- Supporting Information S1

Correspondence to:
D. L. Ficklin,
dficklin@indiana.edu

Citation:
Ficklin, D. L., Abatzoglou, J. T., & Novick, K. A. (2019). A new perspective on terrestrial hydrologic intensity that incorporates atmospheric water demand. *Geophysical Research Letters*, *46*, 8114–8124. https://doi.org/10.1029/2019GL084015

Received 6 JUN 2019
Accepted 6 JUL 2019
Accepted article online 10 JUL 2019
Published online 22 JUL 2019

Abstract Hydrologic intensity is often quantified using precipitation without directly incorporating atmospheric water demand. We develop a hydrologic intensity index called the surplus deficit intensity (SDI) index that accounts for variation in supply and demand. SDI is the standardized sum of standardized surplus intensity (mean of daily surplus when supply > demand) and deficit time (mean of consecutive days when demand > supply). Using an observational ensemble of global daily precipitation and atmospheric water demand during 1979–2017, we document widespread hydrologic intensification (SDI; +0.11 *z*-score per decade) driven primarily by increased surplus intensity. Using a climate model ensemble of the United States, hydrologic intensification is projected for the mid-21st century (+0.86 in *z*-score compared to 1971–2000), producing greater apparent intensification when compared to an index that does not explicitly incorporate demand. While incorporating demand had a minor effect on observed hydrologic intensification, it doubles hydrological intensification for the mid-21st century.

Plain Language Summary Increasing air temperatures have resulted in an intensification, or acceleration, of the terrestrial hydrologic cycle, which is defined as an increase of the water fluxes (precipitation and evapotranspiration) between the surface and the atmosphere. Efforts to quantify hydrologic intensification have traditionally only considered "supply" variables such as precipitation rates without considering "demand" that varies over space and time. For this work we develop a method to quantify hydrologic intensification using supply and demand. This approach shows widespread hydrologic intensification from 1979–2017 across much of the global land surface, which is expected to continue into the future. We additionally compare this new method to a previously developed method that uses only supply without explicitly incorporating demand. Incorporating demand results in a notable hydrologic intensification compared to methods that only use supply or a simplified representation of supply and demand. This work suggests that demand needs to be considered when quantifying hydrologic intensification.

1. Introduction

Climate change is expected to intensify, or accelerate, the hydrologic cycle, defined as an increase in the freshwater flux of water between the atmosphere and land/ocean surface. Increased precipitation, and in particular increased incidence of extreme precipitation, can impair plant function and drive increased runoff rates, leading to greater flood severity and frequency (Huntington, 2006). At the same time, contemporaneous increases in evapotranspiration can cause soil moisture deficits to develop more quickly between precipitation events.

In recent years, substantial effort has been made to develop holistic metrics that quantify the rate of hydrologic intensification (e.g., Giorgi et al., 2011; Gloor et al., 2013; Huntington et al., 2018). Using observations, these metrics suggest that the intensification of the hydrologic cycle is already underway (Barbero et al., 2017; Westra et al., 2013). These metrics are useful heuristics for understanding how climate change can impact a range of variables (i.e., precipitation surpluses and drought) that impact natural ecosystems and socioeconomic systems, often deleteriously. However, most of these existing studies have primarily focused on supply-side hydrologic intensification by examining changes in precipitation characteristics (Giorgi et al., 2011; Gloor et al., 2013; Wu et al., 2013), including the length of dry spells and their resulting effects on other hydrologic components (Alfieri et al., 2017; Déry et al., 2009; Huntington, 2006). This focus on the "supply" side of the cycle, while common in the hydrology literature (Fisher et al., 2017), does not account for changes in atmospheric demand, which has historically increased and is expected to continue to increase under

climate change (Ficklin & Novick, 2017; Greve & Seneviratne, 2015; Milly & Dunne, 2016; Novick et al., 2016; Trenberth et al., 2014).

Considering demand when quantifying hydrologic intensification provides a more balanced seasonal, geographic, and temporally varying view of water fluxes, allowing for a more direct link between intensity metrics and associated water resources and agricultural impacts. If supply and demand increase in a coordinated fashion and at similar magnitudes, high atmospheric demand or potential evapotranspiration will accelerate the rate at which excess supply is returned to the atmosphere where surface water is not limiting (Seneviratne et al., 2010) such that the actual effect on soil moisture and/or streamflow may be relatively small. On the other hand, increased supply during periods when demand is low can lead to saturated soils, flooding (Arnell & Gosling, 2016), and crop loss (Lesk et al., 2016). Increased demand without a coincident change in supply can increase the severity and duration of dry spells, leading to more rapid soil moisture depletion and a host of ecosystem impacts (Abatzoglou & Williams, 2016; McDowell et al., 2008; Sulman et al., 2016; Williams et al., 2013). These scenarios would not be well diagnosed by a supply-only approach for intensification; intensification metrics that consider temporally and spatially varying demand are more closely coupled to ecohydrologic conditions at the land surface and how they change over the subannual timescales at which hydrologic stress evolves and resolves.

While both supply and demand are considered in indices aimed at diagnosing drought (Vicente-Serrano et al., 2010), only a few studies have attempted to account for both supply and demand in hydrologic intensification (Feng et al., 2017; Huntington et al., 2018; Vicente-Serrano et al., 2018); however, these studies relied on proxies for actual evapotranspiration, as opposed to atmospheric demand. Intensity metrics that focus on actual evapotranspiration have many practical uses (Huntington et al., 2018) and may be well suited to capture land-atmosphere feedbacks emerging from plant response to supply and demand (Berg et al., 2016; Oishi et al., 2010; Sulman et al., 2016; Tardieu & Simonneau, 1998; Zhang et al., 2015).

Intensity metrics that rely on atmospheric demand using potential evapotranspiration may better represent the atmosphere's ability to "pull" water from the Earth's surface and are conceptually more closely linked to drought monitoring frameworks (which incorporate information about potential, but not actual, evapotranspiration; Hobbins et al., 2016). Increases in atmospheric demand using observations (Dai, 2011; McAfee, 2013; McCabe & Wolock, 2015; Sheffield et al., 2012) and global climate models (GCMs) have been found (Cook et al., 2014; Scheff & Frierson, 2014), although methods that account for dynamic vegetation responses with elevated atmospheric CO_2, or only the radiative components, moderate such increases (Swann, 2018). No studies, to our knowledge, have considered supply and demand at submonthly time scales in evaluating hydrologic intensification.

This study explores a new hydrological intensity index that uses the magnitude and timing of supply and demand; specifically, we expand upon a preexisting supply-only intensity index proposed by Giorgi et al. (2011) that integrates both precipitation intensity and dry spell length where demand is not explicitly incorporated and does not change over space and time. Many definitions of hydrologic intensification exist in the literature; specifically, we are seeking a methodology and definition that better incorporates the hydrologic cycle balance using supply and demand that varies over space and time. We use this new index to examine the recent character of hydrologic intensification across global terrestrial surfaces from 1979–2017 relative to supply-only indices that do not explicitly incorporate demand. Finally, we additionally explore these differences using an ensemble of climate model output for the contiguous United States.

2. Materials and Methods

2.1. Supply and Demand Index

We develop a hydrological intensity index using supply (precipitation or P) and demand (defined using reference grass evapotranspiration; ET_o) that varies over space and time based on the concept of water surplus ($P > ET_o$) and water deficit ($ET_o > P$) at daily, or equivalent, time scales. It is important to note that we equate demand with atmospheric demand and not necessarily other aspects of hydrologic demand such as groundwater or soil moisture demand. The hydrological intensity index, termed the surplus deficit intensity (or SDI) index, is defined as follows:

$$SDI = \frac{z(\text{SurINT}) + z(\text{DT})}{\text{std}(z(\text{SurINT}) + z(\text{DT}))} \quad (1)$$

where *std* is the standard deviation over the entire time period and z is the standardization of surplus intensity (SurINT) and deficit time (DT). SurINT is defined as the mean surplus ($P - \text{ET}_o$) for days when $P > ET_o$ over each time period—here defined as a calendar year, but scalable to other time periods. SurINT represents the mean daily depth of surplus ($P > ET_o$) for days when $P > ET_o$ over each time period. DT is the mean dry spell length for days when $P < ET_o$ over each time period. Before standardization, DT represents the mean consecutive duration (e.g., in days) when $ET_o > P$. SurINT and DT are standardized (hereafter termed z-score) using their respective base period mean and standard deviation (1979–2017 for observational data and 1971–2000 for the climate model projections) so that the values are centered to have a mean of 0 and scaled to have a standard deviation of 1. A positive (negative) value then indicates a larger (smaller) value compared to the baseline time period. This also allows for spatial comparisons, as every grid point is on the same scale regardless of climate. The use of z-scores can be somewhat abstract, and therefore, we have also added the percent change in SurINT (in millimeter surplus) and DT (in deficit days) when first introducing the results of the new metrics as such measures may be more tangible for understanding impacts. Percent change values of SDI are not shown because it is by definition a combination of standardized values.

Combining both SurINT and DT captures the intensity of surplus events juxtaposed with the overall time in water deficit, defined as SDI. This is different than previous approaches that examine changes in hydroclimatic variability (e.g., wetter wet years and drier dry years; Seager et al., 2012; Swain et al., 2018). A year of anomalously high surplus on wet days ($P > ET_o$) juxtaposed with anomalously high deficit duration (days in a row where $ET_o > P$) would indicate a high SDI (or hydrologically intense) year. As further illustration, a year of intense flooding might not have high SDI because anomalously high surplus (positive SurINT) may not be juxtaposed by a long consecutive duration of demand (negative DT). We summarize the daily data at the annual time step, but other time steps (i.e., standardized seasonal or monthly) can also be assessed.

2.2. Comparison With a Supply-Only Hydrologic Intensity Index

To understand more clearly the impact of incorporating demand into the SDI, we compare SurINT, DT, and SDI with an intensity metric similar to that developed by Giorgi et al. (2011) and further discussed in the hydrologic intensification literature (Giorgi et al., 2014; Huntington et al., 2018). Giorgi et al. (2011) defined the hydrologic intensity (HYINT_GIORGI) index as follows:

$$\text{HYINT\_GIORGI} = \text{INT} * \text{DSL} \quad (2)$$

where INT is the mean annual precipitation intensity (mm) for days where $P > 1$ mm and DSL is the mean number of consecutive days with $P < 1$ mm for a given year in days. Both DSL and INT are normalized by their long-term mean value. A HYINT_GIORGI > 1 indicates a hydrologically intense time period. Giorgi et al. (2011) use 1 mm to distinguish between wet and dry days. Giorgi et al. (2011) is therefore only concerned about the intensity of $P > 1$ mm (defined as INT) and the temporal distance between these precipitation events (DSL). While $P > 1$ mm could simply be interpreted as the threshold for a precipitation event of sufficient depth to infiltrate soil, it also effectively functions as a static-in-time and space minimum atmospheric demand. As an example of using this threshold, we find that globally, on average, terrestrial ET_o exceeds 1 mm 291 days per year for the three ET_o data sets used in this work (see section 2.4 for description of data sets).

Equation (3) below facilitates a direct comparison with SDI, where SurINT and DT are replaced with INT and DSL as written in equation (1).

$$HYINT = \frac{z(\text{INT}) + z(\text{DSL})}{\text{std}(z(\text{INT}) + z(\text{DSL}))} \quad (3)$$

2.3. Physical Description and Advancement of the New Metric

Our metrics (SurINT, DT, and SDI) build upon Giorgi et al.'s (2011) definition of HYINT but explicitly incorporates temporal variability of atmospheric demand. In this case, the balance of two climatic variables (P and ET_o) are used to quantify hydrologic intensification (see Table S1 in the supporting information). Whether or

not demand is considered in the calculation of surplus and DT can have a substantial impact on the magnitude and direction of hydrological intensification. Our approach explicitly recognizes that, as ET_o increases and the atmosphere becomes more desiccating, precipitation will be stored as soil moisture for a shorter period of time, and the land surface may experience drier conditions even if precipitation patterns themselves are stationary. For days when there is a surplus of moisture ($P > ET_o$, herein defined as SurINT), this surplus can replenish soil moisture, groundwater recharge and potentially result in surface runoff. On the other hand, on days when $P < ET_o$ any precipitation that occurs is insufficient to overcome atmospheric evaporative demand, resulting in a deficit of moisture for plant-usable water, soil moisture, and groundwater recharge. As a result, DT is more closely coupled to ecosystem processes than DSL as it reflects the duration over which plant-available water might be limiting and soil moisture/groundwater is being depleted.

Complementary to Giorgi et al. (2011), we combine DT and SurINT in the development of a hydrological intensity index. Climate change is generally projected to result in an increase in intense precipitation with a corresponding increase in atmospheric demand. SDI is able to capture these changes, while metrics such as Giorgi et al. (2011) would only be able to assess the changes in intense precipitation events because demand does not change over time and space. We realize that the comparison between our metrics and Giorgi et al.'s (2011) metrics is not a one-to-one comparison and the definitions of the two metrics may produce differences in the magnitude of hydrologic intensification.

2.4. Supply and Demand Data Sets

An ensemble of global supply and demand data sets were used to diagnose changes in HYINT during 1979–2017. We used an ensemble approach for historical assessments of change to better understand the degree to which changes are robust to structural uncertainty in climate data sets of different provenances, particularly given the notable uncertainty in precipitation trends from different data sets (Beck et al., 2017). We used four global precipitation data sets for historical analyses: Multi-Source Weighted-Ensemble Precipitation Version 2 (MSWEP; Beck et al., 2017), National Centers for Environmental Prediction-National Center for Atmospheric Research reanalysis (NCEP-NCAR; Kalnay et al., 1996), Modern-Era Retrospective Analysis for Research and Applications, Version 2 (MERRA-2; Gelaro et al., 2017), and ERA-Interim reanalysis (ERA-I; Dee et al., 2011). For the demand data sets, we used the American Society of Civil Engineers Penman-Monteith method for a reference grass surface (ET_o; Walter et al., 2000) using daily maximum/minimum temperature, daily mean specific humidity, wind speed, and downward shortwave radiation flux inputs from the National Centers for Environmental Prediction-National Center for Atmospheric Research reanalysis, Modern-Era Retrospective Analysis for Research and Applications, Version 2 reanalysis, and the ERA-Interim reanalysis. This results in an ensemble of 12 total combinations of P and ET_o data sets, all regridded to a common resolution of ~1.87° after hydrologic intensification metrics were calculated at the native resolution of the original data set. These data sets are described in the supporting information. For comparison with Giorgi et al. (2011), we focus on ensemble mean and standard deviation of SurINT, DT, and SDI for each P data set using the three ET_o data sets, resulting in four supply and demand ensemble data sets to be compared with the four P-only data sets used to calculate INT, DSL, and HYINT. Figure S1 displays the ensemble averaging for comparison with Giorgi et al. (2011).

For the projected climate analysis, we used an ensemble of 11 GCMs for the contiguous United States derived from the Coupled Model Intercomparison Project Phase 5 (Taylor et al., 2012), which can be found in Table S2. Data were considered for two time periods: (a) 1971–2000 for historical forcing and (b) 2041–2070 for RCP8.5 forcing. GCM output was bilinearly interpolated from their native resolution to a common 1° resolution grid.

2.5. Statistical Analyses

We examine SDI and HYINT metrics for each grid point and their trends during 1979–2017 using the Sen-Theil slope estimator (Sen, 1968; Theil, 1992) and the Mann-Kendall trend test (Kendall, 1975; Mann, 1945) for trend significance at $p < 0.05$. It is important to note that the trend estimates should be interpreted with caution as gridded data sets may be prone to inhomogeneities that can lead to spurious trends (Beck, van Dijk, et al., 2017; Maidment et al., 2015), thus prompting our analysis of trends using several different data sets. For the projected climate data, we calculated z-score differences for the mid-21st century (2041–2070) relative to the late twentieth century (1971–2000) for the SDI and HYINT metrics.

Trends for all supply and demand combinations for the historical time period and projected changes for each GCM are found in the supporting information. To address the uncertainty of the input data sets, we present the ensemble mean, ensemble variability, and the fraction of terrestrial area that contains significant increases and decreases. To capture statistical significance of the trends, we also summarize the ensemble significance by presenting the number of data sets (12 for SDI and its individual components and 4 for HYINT and its individual components) that agree on significance for each grid point.

3. Results and Discussion

3.1. Temporal and Spatial Variability in Historic SurINT, DT, and SDI

The ensemble spatial mean of SurINT increased from 1979–2017 by +0.11 z-score per decade (2.2 % increase per decade in surplus; Figure S2) for terrestrial surfaces (Figures 1, 2, S2, and S3). The fraction of terrestrial area with a significant increase ranged from 0.15 to 0.3 compared to <0.1 for areas with a significant decrease (Figure 2). The largest increases occurred in central South America (0.34 z-score per decade; 6.7% increase per decade in surplus; Figure S2) and southern Africa (0.12 z-score per decade; 7.6% increase per decade in surplus; Figure S2) with strong ensemble agreement in these regions (Figures 1 and S4). Decreased SurINT were detected in portions of western North America, Europe, central Africa, and Asia, although the magnitudes of the declines were relatively small (compared to the areas where SurINT increased).

We find a nominal increase of +0.01 z-score per decade for DT over terrestrial surfaces (1.12 % increase in deficit days per decade; Figure S2), with no clear agreement among the ensemble (Figures 1, 2, and S5). We find nearly equal fractional areas of significant increases and decreases, with an overall ensemble range of 0.05 to 0.23 for significant increases and 0.08 to 0.18 for significant decreases (Figure 2). The most significant and largest agreement of significance was found in central Africa (ensemble mean of 0.14 z-score per decade; 3.3% increase per decade in deficit days; Figure S2), western North America (0.19 z-score per decade; 4.6% increase per decade in deficit days; Figure S2), and throughout Europe and Asia (Figure 1, Figure S5). The largest decreases in DT occurred in southern (as well as portions of eastern and western) Africa, northern North America, northern South America, and portions of central Asia (Figure 1 and Figure S4–S5).

The confluence of observed trends in ensemble mean SurINT and DT drove an increase ensemble average increase in SDI with a trend of +0.11 z-score per decade and an ensemble range of +0.025 to +0.15 (Figures 1, 2, and S6). We also find more fractional area of significant increases (ensemble range 0.8 to 0.28) than significant decreases (<0.10; Figure 2). SDI increased for all continents, but the largest increases were located where both SurINT and DT increased, namely, central Africa, the western United States, South America, and central/northern Asia (Figure 1).

3.2. Comparison of Recent Climate Trends With a Supply-Only Intensity Metric

The surplus metrics (SurINT and INT) showed similar patterns and magnitude of trends, and fractional areas of significant change for 1979–2017 (Figures 2, S2, and S7–S9). The ensemble spatial average trends were also similar on the deficit side of the intensity question but with an overall larger area of significant increases of DT compared to DSL (Figure 2). This result is consistent with steady or decreasing P (Figure S10) with an overall increase ET_o, but also seasonal and geographic changes (Figure S11), resulting in more P events failing to exceed ET_o. Differences in these changes resulted in differences in SDI and HYINT, with an overall larger increase in SDI (+0.11 z-score per decade) as compared to HYINT (+0.07 z-score per decade).

The spatial patterns between trends in the SDI and HYINT metrics and their components were also similar (Figure S7) and further indicated by strong Pearson correlations between terrestrial spatial trends in SurINT and INT (0.92), DT and DSL (0.80), and SDI and HYINT (0.76). Noticeable differences can be found, however. Trends in SurINT and DT were overall larger than INT and DSL, though the differences were nominal (Figures S7 and 2). DT for several regions (western United States, central Africa, and much of Asia) were larger than the trends in DSL, with much of this area having also experienced increasing ET_o (Figure S11), which is not accounted for in the Giorgi et al. (2011) intensity metric. More widespread decreases in DSL were observed in the Southern Hemisphere, a result that is likely linked to widespread increases in P and/or decreases in ET_o (Figures S10 and S11).

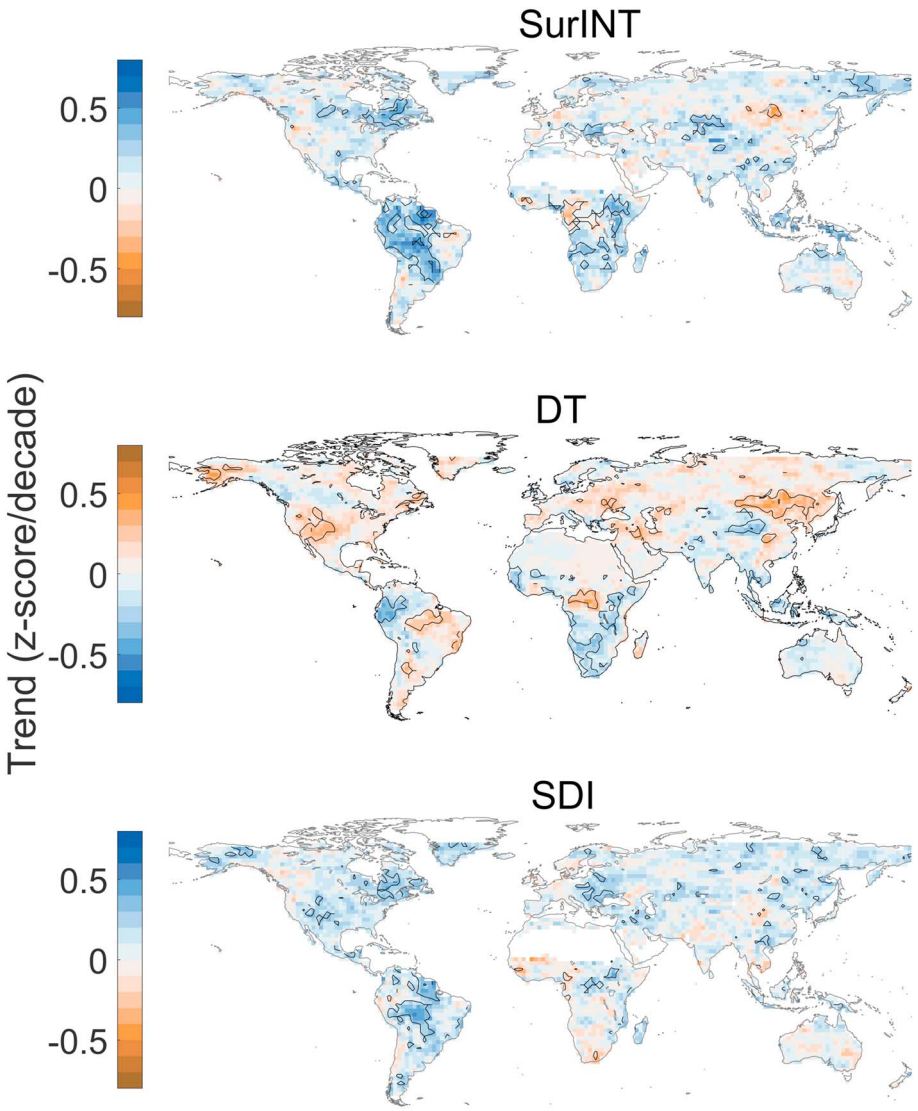

Figure 1. Ensemble mean trends in hydrological intensification using indices with supply and demand (surplus intensity [SurINT], deficit time [DT], and surplus deficit intensity [SDI]) during 1979–2017 expressed in units of z-score per decade.

While the definition of intensification is different, the incorporation of temporally and spatially varying demand to quantify intensification becomes clearer when considering trends in precipitation and ET_o (Figures S10 and S11; correlations found in Table S3). Specifically, we decompose the relationship between trends during 1979–2017 in P and ET_o into four quadrants corresponding to bivariate increases and decreases in P and ET_o (Figure S12). For the historical climate, we find that larger trends in INT, DSL, and HYINT compared to SurINT, DT, and SDI are found in quadrants where ET_o decreased. More positive trends for metrics that incorporate demand are found in quadrants where ET_o increased (Figure S12). This indicates that explicitly considering demand that varies will generally lead to more positive hydrologic intensification trends ($r = 0.17$ between SDI minus HYINT and ET_o trend), consistent with the conceptual scenarios presented in Table S1.

3.3. Comparison of Projected Climate Trends With a Supply-Only Intensity Metric

For the GCM ensemble, SDI shows stronger and more widespread hydrologic intensification by midcentury across the continental United States (ensemble mean z-score of +0.86 with intermodel range of +0.6 to +1.25) than HYINT (z-score of +0.47 with intermodel range of +0.1 to +0.95; Figures 2, 3, and S13) as a result of changes in their individual components (Figures S14–S19). The fraction of area with a significant

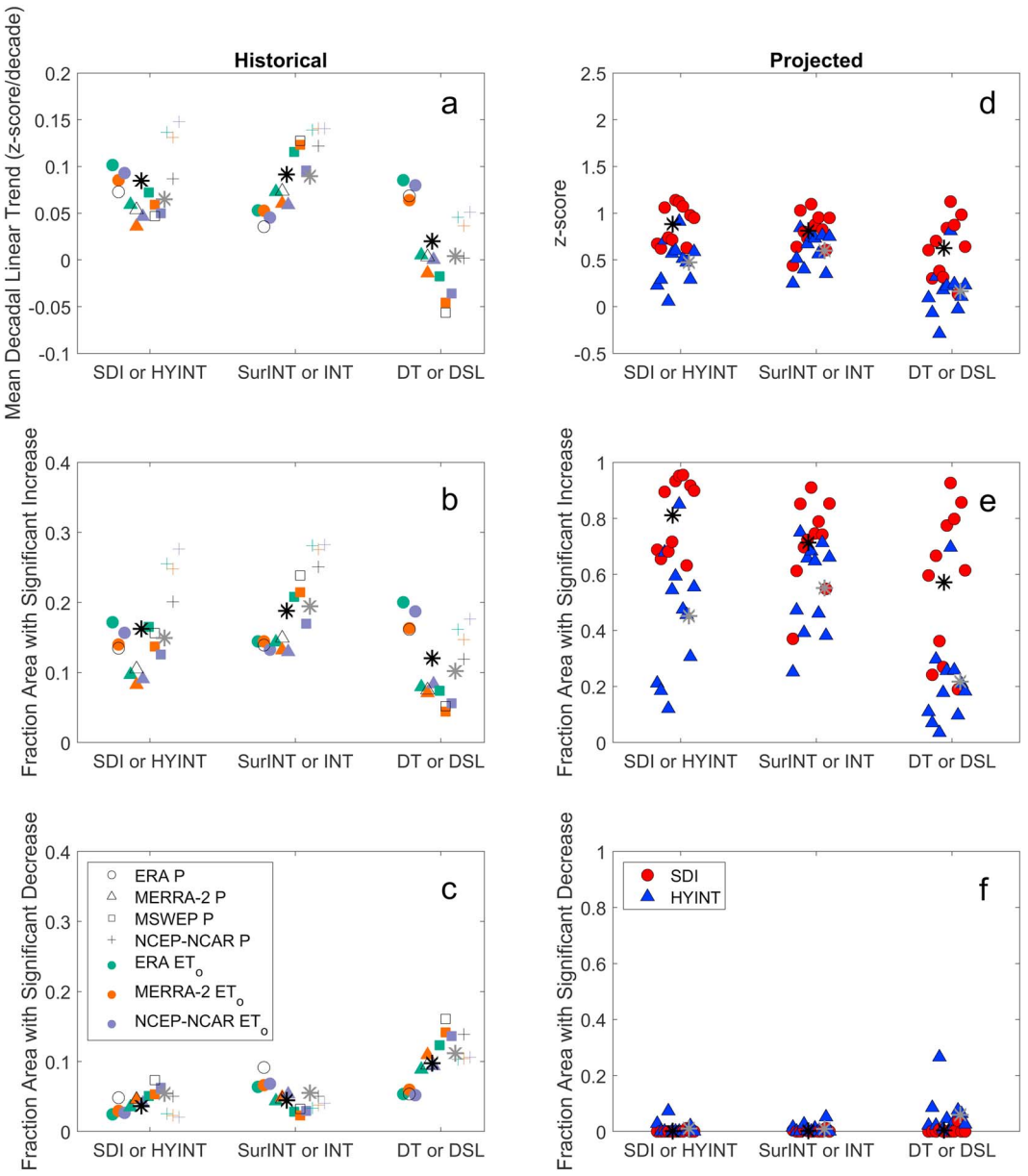

Figure 2. (a) Area-weighted global mean trends in hydrologic intensity metrics during 1979–2017, (b) the fraction of area with significant ($p < 0.05$) increases, and (c) significant decreases. (d–f) Area-weighted projected changes for 2041–2070 relative to 1971–2000 period for the contiguous United States. Hydrologic intensity metrics that incorporate supply and demand include surplus intensity (SurINT), deficit time (DT), and surplus deficit intensity (SDI), while supply and static demand intensity metrics include precipitation intensity (INT), dry spell length (DSL), and hydrologic intensity (HYINT) from Giorgi et al. (2011). The filled symbols for panels (a)–(c) indicate combinations of precipitation (P) and reference evapotranspiration (ET_o) from various data sets, while the hollow symbols indicate the supply-only hydrologic intensity calculations. For the projected time period, the filled circles indicate an individual global climate model projection for the supply and demand intensity metric, while the filled triangles indicate an individual global climate model projection for the supply-only intensity metric. Black asterisks represent the ensemble mean of supply and demand intensity metrics, while the grey asterisks represent the ensemble mean of the supply-only intensity metrics.

increase for SDI ranged from 0.75 to nearly 1.0, while the fraction ranged from 0.2 to 0.92 for HYINT (Figure 2). Both metrics had a fraction of area with a significant decrease less than 0.1. Widespread increases were found in both SurINT and INT (Figures 2, 3, and S13), with an overall larger mean ensemble z-score in SurINT (z-score of +0.79) compared to INT (z-score of +0.56). Additionally, increases

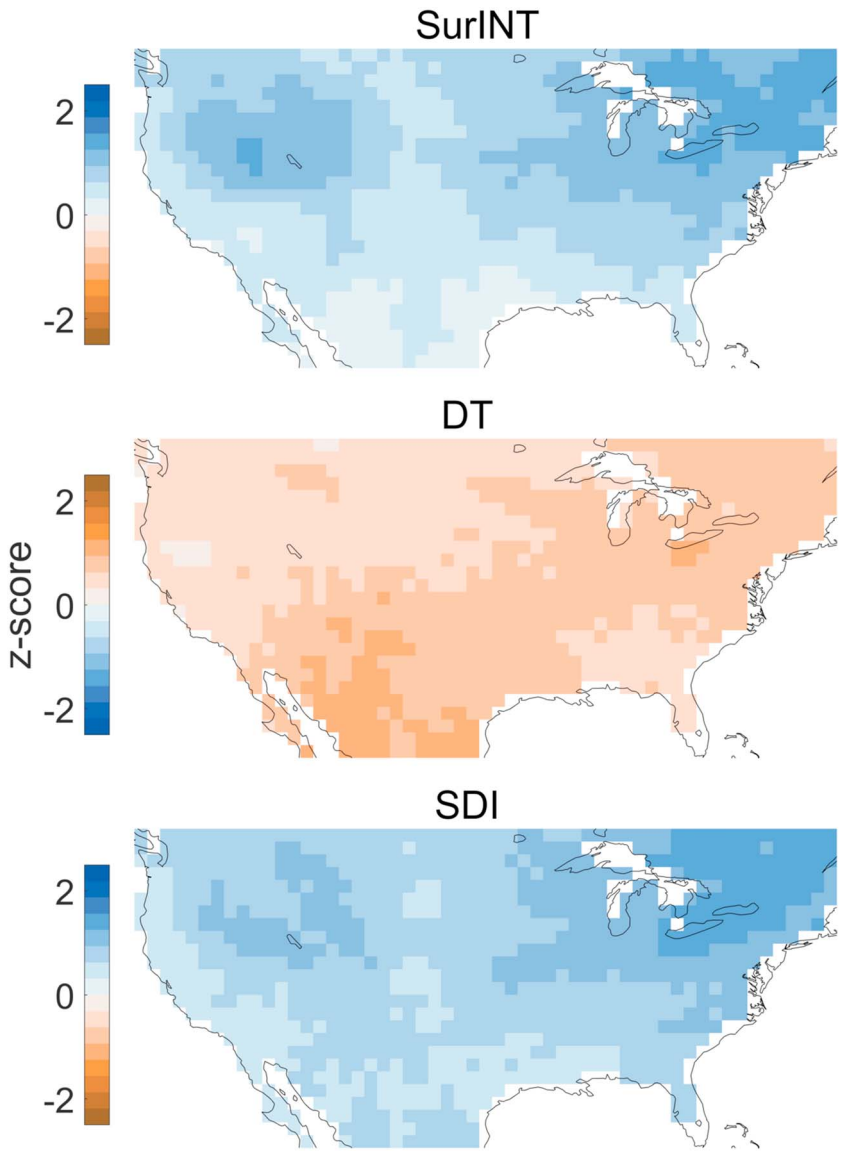

Figure 3. Multimodel mean *z*-scores of hydrological intensification using indices with supply and demand (surplus intensity [SurINT], deficit time [DT], and surplus deficit intensity [SDI]) for 2041–2070 from 11 global climate models (see Table S1). The baseline time period for standardization is 1971–2010.

in DT were much larger (ensemble mean *z*-score of +0.64) compared to DSL (*z*-score of +0.19) and is further shown by their fraction of significant increase and decrease (Figure 2).

Compared to the historical time period, DT becomes a larger component of hydrologic intensification for the future time period. This phenomenon is largely explained by increased ET_o from temperature-driven increases in vapor pressure deficit, which is not accounted for with a static 1-mm demand term implicit in the Giorgi et al. (2011) index. As a result, in the future, consecutive days when $ET_o > P$ occur more frequently. Our results are consistent with projected future increases in an aridity index assessed on longer timescales (P/ET_o; Scheff & Frierson, 2015), but our study is uniquely focused on the balance of P and ET_o at timescales over which hydrologic stress often evolve and resolve. Despite the clear role of increased DT in driving the future intensification, it is important to note that SurINT is also projected to increase in the future. Chou et al. (2013) also support this finding using historical data, showing that the historical annual range of precipitation has increased where wetter seasons have become wetter and drier seasons have become drier. Likewise, models generally project increased precipitation intensity along with more

days with low precipitation (Polade et al., 2013) that in conjunction with increased ET_o would favor hydrologic intensification. Finally, land surface feedbacks including increased water use efficiency under elevated CO_2 and changes in leaf area and biomass can be important regulators of how the actual ET rates that drive the hydrologic cycle forward. Linking our results to these specific mechanisms is beyond the scope of this paper, though we note that our results reflect these processes as they are represented in the land surface that inform the Coupled Model Intercomparison Project model projections for future ET_o and precipitation (Berg et al., 2016; Swann, 2018).

These projected changes in intensification are linked to projected changes in P (Figure S20) and ET_o (Figure S21) across the continental United States. Average mean annual P increases of +0.36 z-score for the GCM ensemble mean and significant increases in projected ET_o of +2.4 z-score are found, a result also found in Greve and Seneviratne (2015). Explicit inclusion of a demand component in HYINT metrics that varies over space and time resulted in a larger increase in intensity in regions where ET_o is projected to increase regardless of projected changes in P (Figure S12). Hydrologic intensification using demand is higher for nearly every grid point as compared to hydrologic intensification for supply-only approaches (Figures S12 and S13).

4. Conclusions

We expand upon previous HYINT work of Giorgi et al. (2011) by explicitly incorporating a temporally and spatially varying demand (ET_o) term. Using this new perspective, we find widespread hydrologic intensification across global terrestrial surface from 1979–2017 with slightly larger rates of intensification and broader geographic extent than analogous approaches that consider supply and simplified demand terms. Including a demand term that varies over space and time shifts the definition of HYINT toward a perspective more closely linked to ecohydrologic conditions at the land surface and thus provides an informative comparison that may be useful when considering the impacts of HYINT. Using an ensemble of climate projections of the mid-21st century, we show that this new perspective results in more notable increases in HYINT across the continental United States than supply-only indices. This is in large part due to the widespread increases in ET_o, where larger demand will cause fewer precipitation events to meet the P-ET_o threshold, thereby increasing the DT.

There is good evidence that the hydrologic cycle has been intensifying, which is leading to an increase in juxtaposed hydrologic extremes such as droughts or floods (Zolina et al., 2013; Zscheischler et al., 2018), which is further confirmed by this work. Most often, hydrologic intensification is assessed by quantifying changes in precipitation without the influence of increasing atmospheric demand. We show that including demand results in more widespread hydrologic intensification than indicated by previous metrics, especially under climate change. When considering the consequences of hydrological intensification for human and natural systems, especially under climate change, the evolution of the balance between supply and demand must be considered.

Acknowledgments
We acknowledge the World Climate Research Programme's Working Group on Coupled Modelling, which is responsible for the Coupled Model Intercomparison Project (CMIP). The MSWEP data are available via the http://www.gloh2o.org/ website. The NCEP-NCAR data are available via the ESRL website (https://www.esrl.noaa.gov/psd/data/gridded/data.ncep.reanalysis.html). The MERRA-2 data are available via the GMAO website (https://gmao.gsfc.nasa.gov/reanalysis/MERRA-2/). The ERA-I data are available via the ECMWF website (https://www.ecmwf.int/en/forecasts/datasets/reanalysis-datasets/era-interim). Sample code to calculate SurINT, DT, and SDI can be found on GitHub (https://github.com/dficklin/Ficklin_etal_GRL_SDI). The authors declare no conflict of interests.

References

Abatzoglou, J. T., & Williams, A. P. (2016). Impact of anthropogenic climate change on wildfire across western US forests. *Proceedings of the National Academy of Sciences*, *113*(42), 11,770–11,775. http://www.pnas.org/content/pnas/113/42/11770.full.pdf, https://doi.org/10.1073/pnas.1607171113

Alfieri, L., Bisselink, B., Dottori, F., Naumann, G., Roo, A., Salamon, P., et al. (2017). Global projections of river flood risk in a warmer world. *Earth's Future*, *5*, 171–182. https://doi.org/10.1002/2016EF000485

Arnell, N. W., & Gosling, S. N. (2016). The impacts of climate change on river flood risk at the global scale. *Climatic Change*, *134*(3), 387–401 . https://doi.org/10.1007/s10584-014-1084-5

Barbero, R., Fowler, H. J., Lenderink, G., & Blenkinsop, S. (2017). Is the intensification of precipitation extremes with global warming better detected at hourly than daily resolutions? *Geophysical Research Letters*, *44*, 974–983. https://doi.org/10.1002/2016GL071917

Beck, H. E., van Dijk, A. I. J. M., Levizzani, V., Schellekens, J., Miralles, D. G., Martens, B., & de Roo, A. (2017). MSWEP: 3-hourly 0.25° global gridded precipitation (1979–2015) by merging gauge, satellite, and reanalysis data. *Hydrology and Earth System Sciences*, *21*(1), 589–615. https://doi.org/10.5194/hess-21-589-2017

Beck, H. E., Vergopolan, N., Pan, M., Levizzani, V., van Dijk, A. I. J. M., Weedon, G. P., et al. (2017). Global-scale evaluation of 22 precipitation datasets using gauge observations and hydrological modeling. *Hydrology and Earth System Sciences*, *21*(12), 6201–6217. https://doi.org/10.5194/hess-21-6201-2017

Berg, A., Findell, K., Lintner, B., Giannini, A., Seneviratne, S. I., Van den Hurk, B., et al. (2016). Land–atmosphere feedbacks amplify aridity increase over land under global warming. *Nature Climate Change*, *6*(9), 869–874. https://doi.org/10.1038/nclimate3029

Chou, C., Chiang, J. C. H., Lan, C.-W., Chung, C.-H., Liao, Y.-C., & Lee, C.-J. (2013). Increase in the range between wet and dry season precipitation. *Nature Geoscience*, *6*(4), 263–267. https://doi.org/10.1038/ngeo1744

Cook, B., Smerdon, J., Seager, R., & Coats, S. (2014). Global warming and 21st century drying. *Climate Dynamics*, *43*(9-10), 2607–2627. https://doi.org/10.1007/s00382-014-2075-y

Dai, A. (2011). Drought under global warming: A review. *Wiley Interdisciplinary Reviews: Climate Change*, *2*(1), 45–65. https://doi.org/10.1002/wcc.81

Dee, D. P., Uppala, S. M., Simmons, A. J., Berrisford, P., Poli, P., Kobayashi, S., et al. (2011). The ERA-Interim reanalysis: Configuration and performance of the data assimilation system. *Quarterly Journal of the Royal Meteorological Society*, *137*(656), 553–597. https://doi.org/10.1002/qj.828

Déry, S. J., Hernández-Henríquez, M. A., Burford, J. E., & Wood, E. F. (2009). Observational evidence of an intensifying hydrological cycle in northern Canada. *Geophysical Research Letters*, *36*, L13402. https://doi.org/10.1029/2009GL038852

Feng, H., Zou, B., & Luo, J. (2017). Coverage-dependent amplifiers of vegetation change on global water cycle dynamics. *Journal of Hydrology*, *550*, 220–229. https://doi.org/10.1016/j.jhydrol.2017.04.056

Ficklin, D. L., & Novick, K. A. (2017). Historic and projected changes in vapor pressure deficit suggest a continental-scale drying of the United States atmosphere. *Journal of Geophysical Research: Atmospheres*, *122*, 2061–2079. https://doi.org/10.1002/2016JD025855

Fisher, J. B., Melton, F., Middleton, E., Hain, C., Anderson, M., Allen, R., et al. (2017). The future of evapotranspiration: Global requirements for ecosystem functioning, carbon and climate feedbacks, agricultural management, and water resources. *Water Resources Research*, *53*, 2618–2626. https://doi.org/10.1002/2016WR020175

Gelaro, R., McCarty, W., Suárez, M. J., Todling, R., Molod, A., Takacs, L., et al. (2017). The Modern-Era Retrospective Analysis for Research and Applications, Version 2 (MERRA-2). *Journal of Climate*, *30*(14), 5419–5454. https://doi.org/10.1175/JCLI-D-16-0758.1

Giorgi, F., Coppola, E., & Raffaele, F. (2014). A consistent picture of the hydroclimatic response to global warming from multiple indices: Models and observations. *Journal of Geophysical Research: Atmospheres*, *119*, 11,695–611,708. https://doi.org/10.1002/2014JD022238

Giorgi, F., Im, E.-S., Coppola, E., Diffenbaugh, N. S., Gao, X. J., Mariotti, L., & Shi, Y. (2011). Higher hydroclimatic intensity with global warming. *Journal of Climate*, *24*(20), 5309–5324. https://doi.org/10.1175/2011JCLI3979.1

Gloor, M., Brienen, R. J. W., Galbraith, D., Feldpausch, T. R., Schöngart, J., Guyot, J.-L., et al. (2013). Intensification of the Amazon hydrological cycle over the last two decades. *Geophysical Research Letters*, *40*, 1729–1733. https://doi.org/10.1002/grl.50377

Greve, P., & Seneviratne, S. I. (2015). Assessment of future changes in water availability and aridity. *Geophysical Research Letters*, *42*, 5493–5499. https://doi.org/10.1002/2015GL064127

Hobbins, M. T., Wood, A., McEvoy, D. J., Huntington, J. L., Morton, C., Anderson, M., & Hain, C. (2016). The evaporative demand drought index. Part I: Linking drought evolution to variations in evaporative demand. *Journal of Hydrometeorology*, *17*(6), 1745–1761. https://doi.org/10.1175/JHM-D-15-0121.1

Huntington, T. G. (2006). Evidence for intensification of the global water cycle: Review and synthesis. *Journal of Hydrology*, *319*(1-4), 83–95. https://doi.org/10.1016/j.jhydrol.2005.07.003

Huntington, T. G., Weiskel, P. K., Wolock, D. M., & McCabe, G. J. (2018). A new indicator framework for quantifying the intensity of the terrestrial water cycle. *Journal of Hydrology*, *559*, 361–372. https://doi.org/10.1016/j.jhydrol.2018.02.048

Kalnay, E., Kanamitsu, M., Kistler, R., Collins, W., Deaven, D., Gandin, L., et al. (1996). The NCEP/NCAR 40-year reanalysis project. *Bulletin of the American Meteorological Society*, *77*(3), 437–471. https://doi.org/10.1175/1520-0477(1996)077<0437:TNYRP>2.0.CO;2

Kendall, M. G. (1975). *Rank correlation methods*. London: Griffin.

Lesk, C., Rowhani, P., & Ramankutty, N. (2016). Influence of extreme weather disasters on global crop production. *Nature*, *529*(7584), 84–87. https://doi.org/10.1038/nature16467

Maidment, R. I., Allan, R. P., & Black, E. (2015). Recent observed and simulated changes in precipiation over Africa. *Geophysial Research Letters*, *42*, 8155–8164. https://doi.org/10.1002/2015GL065765

Mann, H. B. (1945). Nonparametric tests against trend. *Econometrica*, *13*(3), 245–259. https://doi.org/10.2307/1907187

McAfee, S. (2013). Methodological differences in projected potential evapotranspiration. *Climatic Change*, *120*(4), 915–930. https://doi.org/10.1007/s10584-013-0864-7

McCabe, G. J., & Wolock, D. M. (2015). Variability and trends in global drought. *Earth and Space Science*, *2*, 223–228. https://doi.org/10.1002/2015EA000100

McDowell, N., Pockman, W. T., Allen, C. D., Breshears, D. D., Cobb, N., Kolb, T., et al. (2008). Mechanisms of plant survival and mortality during drought: Why do some plants survive while others succumb to drought. *New Phytologist*, *178*(4), 719–739. https://doi.org/10.1111/j.1469-8137.2008.02436.x

Milly, P. C. D., & Dunne, K. A. (2016). Potential evapotranspiration and continental drying. *Nature Climate Change*, *6*(10), 946–949. https://doi.org/10.1038/nclimate3046

Novick, K. A., Ficklin, D. L., Stoy, P. C., Williams, C. A., Bohrer, G., Oishi, A. C., et al. (2016). The increasing importance of atmospheric demand for ecosystem water and carbon fluxes. *Nature Climate Change*, *6*(11), 1023–1027. https://doi.org/10.1038/nclimate3114

Oishi, A. C., Oren, R., Novick, K. A., Palmroth, S., & Katul, G. G. (2010). Interannual invariability of forest evapotranspiration and its consequence to water flow downstream. *Ecosystems*, *13*(3), 421–436. https://doi.org/10.1007/s10021-010-9328-3

Polade, S. D., Gershunov, A., Cayan, D. R., Dettinger, M. D., & Pierce, D. W. (2013). Natural climate variability and teleconnections to precipitation over thePacific-North American region in CMIP3 and CMIP5 models. *Geophysical Research Letters*, *40*, 2296–2301. https://doi.org/10.1002/grl.50491

Scheff, J., & Frierson, D. M. W. (2014). Scaling potential evapotranspiration with greenhouse warming. *Journal of Climate*, *27*(4), 1539–1558. https://doi.org/10.1175/JCLI-D-13-00233.1

Scheff, J., & Frierson, D. M. W. (2015). Terrestrial aridity and its response to greenhouse warming across CMIP5 climate models. *Journal of Climate*, *28*(14), 5583–5600. https://doi.org/10.1175/JCLI-D-14-00480.1

Seager, R., Naik, N., & Vogel, L. (2012). Does Global Warming Cause Intensified Interannual Hydroclimate Variability?, *Journal of Climate 25*(9), 3355–3372. https://doi.org/10.1175/JCLI-D-11-00363.1

Sen, P. K. (1968). Estimates of the regression coefficient based on Kendall's Tau. *Journal of the American Statistical Association*, *63*(324), 1379–1389. https://doi.org/10.1080/01621459.1968.10480934

Seneviratne, S. I., Corti, T., Davin, E. L., Hirschi, M., Jaeger, E. B., Lehner, I., et al. (2010). Investigating soil moisture–climate interactions in a changing climate: A review. *Earth-Science Reviews*, *99*(3-4), 125–161. http://www.sciencedirect.com/science/article/pii/S0012825210000139, https://doi.org/10.1016/j.earscirev.2010.02.004

Sheffield, J., Wood, E. F., & Roderick, M. L. (2012). Little change in global drought over the past 60 years. *Nature*, *491*(7424), 435–438. https://doi.org/10.1038/nature11575

Sulman, B. N., Roman, D. T., Yi, K., Wang, L., Phillips, R. P., & Novick, K. A. (2016). High atmospheric demand for water can limit forest carbon uptake and transpiration as severely as dry soil. *Geophysical Research Letters*, *43*, 9686–9695. https://doi.org/10.1002/2016GL069416

Swain, D. L., Langenbrunner, B., Neelin, J. D., & Hall, A. (2018). Increasing precipitation volatility in twenty-first century California. *Nature Climate Change*, *8*(5), 427–433. https://doi.org/10.1038/s41558-018-0140-y

Swann, A. L. S. (2018). Plants and drought in a changing climate. *Current Climate Change Reports*, *4*(2), 192–201. https://doi.org/10.1007/s40641-018-0097-y

Tardieu, F., & Simonneau, T. (1998). Variability among species of stomatal control under fluctuating soil water status and evaporative demand: Modelling isohydric and anisohydric behaviours. *Journal of Experimental Botany*, *49*(Special), 419–432. https://doi.org/10.1093/jxb/49.Special_Issue.419

Taylor, K. E., Stouffer, R. J., & Meehl, G. A. (2012). An overview of CMIP5 and the experiment design. *Bulletin of the American Meteorological Society*, *93*(4), 485–498. https://doi.org/10.1175/BAMS-D-11-00094.1

Theil, H. (1992). A rank-invariant method of linear and polynomial regression analysis. In B. Raj, & J. Koerts (Eds.), *Henri Theil's contributions to economics and econometrics: Econometric theory and methodology*, (pp. 345–381). Dordrecht: Springer Netherlands. https://doi.org/10.1007/978-94-011-2546-8_20

Trenberth, K. E., Dai, A., van der Schrier, G., Jones, P. D., Barichivich, J., Briffa, K. R., & Sheffield, J. (2014). Global warming and changes in drought. *Nature Climate Change*, *4*(1), 17–22. https://doi.org/10.1038/nclimate2067

Vicente-Serrano, S. M., Beguería, S., & López-Moreno, J. I. (2010). A multiscalar drought index sensitive to global warming: The standardized precipitation evapotranspiration index. *Journal of Climate*, *23*(7), 1696–1718. https://doi.org/10.1175/2009JCLI2909.1

Vicente-Serrano, S. M., Miralles, D. G., Domínguez-Castro, F., Azorin-Molina, C., el Kenawy, A., McVicar, T. R., et al. (2018). Global assessment of the standardized evapotranspiration deficit index (SEDI) for drought analysis and monitoring. *Journal of Climate*, *31*(14), 5371–5393. https://doi.org/10.1175/JCLI-D-17-0775.1

Walter, I. A., Allen, R. G., Elliott, R., Jensen, M., Itenfisu, D., Mecham, B., Howell, T., Snyder, R., Brown, P, & Echings, S. (2000). ASCE's standardized reference evapotranspiration equation. In Watershed management and operations management 2000 (pp. 1–11).

Westra, S., Alexander, L. V., & Zwiers, F. W. (2013). Global increasing trends in annual maximum daily precipitation. *Journal of Climate*, *26*(11), 3904–3918. https://doi.org/10.1175/JCLI-D-12-00502.1

Williams, A. P., Allen, C. D., Macalady, A. K., Griffin, D., Woodhouse, C. A., Meko, D. M., et al. (2013). Temperature as a potent driver of regional forest drought stress and tree mortality. *Nature Climate Change*, *3*(3), 292–297. https://doi.org/10.1038/nclimate1693

Wu, P., Christidis, N., & Stott, P. (2013). Anthropogenic impact on Earth's hydrological cycle. *Nature Climate Change*, *3*(9), 807–810. https://doi.org/10.1038/nclimate1932

Zhang, K., Kimball, J. S., Nemani, R. R., Running, S. W., Hong, Y., Gourley, J. J., & Yu, Z. (2015). Vegetation greening and climate change promote multidecadal rises of global land evapotranspiration. *Scientific Reports*, *5*(1). https://doi.org/10.1038/srep15956

Zolina, O., Simmer, C., Belyaev, K., Gulev, S. K., & Koltermann, P. (2013). Changes in the duration of European wet and dry spells during the last 60 years. *Journal of Climate*, *26*(6), 2022–2047. https://doi.org/10.1175/JCLI-D-11-00498.1

Zscheischler, J., Westra, S., van den Hurk, B. J. J. M., Seneviratne, S. I., Ward, P. J., Pitman, A., et al. (2018). Future climate risk from compound events. *Nature Climate Change*, *8*(6), 469–477. https://doi.org/10.1038/s41558-018-0156-3